Low concentrations of near-surface ozone in Siberia

Ann-Christine Engvall Stjernberg Engvall Stjernberg, A. Skorokhod, J.D. Paris, N. Elansky, P. Nédélec & A. Stohl

Low concentrations of near-surface ozone in Siberia

By ANN-CHRISTINE ENGVALL STJERNBERG[1,2]*, A. SKOROKHOD[3], J. D. PARIS[4], N. ELANSKY[3], P. NÉDÉLEC[5] and A. STOHL[1], [1]*Norwegian Institute for Air Research, Kjeller, Norway;* [2]*Department of Applied Environmental Science, Stockholm University, Stockholm, Sweden;* [3]*Obukhov Institute for Atmospheric Physics, Moscow, Russia;* [4]*Laboratorie des Sciences du Climat et de l'Environnment, Gif sur Yvette, France;* [5]*Laboratorie d'Aérologie, Toulouse, France*

ABSTRACT

Siberia with its large area covered with boreal forests, wetlands and tundra is believed to be an important sink for ozone via dry deposition and reactions with biogenic volatile organic compounds (BVOCs) emitted by the forests. To study the importance of deposition of ozone in Siberia, we analyse measurements of ozone mixing ratios taken along the Trans-Siberian railway by train, air-borne measurements and point measurements at the Zotino station. For all data, we ran the Lagrangian particle dispersion model FLEXPART in backward mode for 20 d, which yields the so-called potential emission sensitivity (PES) fields. These fields give a quantitative measure of where and how strongly the sampled air masses have been in contact with the surface and hence possible influenced by surface fluxes. These fields are further statistically analysed to identify source and sink regions that are influencing the observed ozone. Results show that the source regions for the surface ozone in Siberia are located at lower latitudes: the regions around the Mediterranean Sea, the Middle East, Kazakhstan and China. Low ozone mixing ratios are associated to transport from North West Russia, the Arctic region, and the Pacific Ocean. By calculating PES values for both a passive tracer without consideration of removal processes and for an ozone-like tracer where dry deposition processes are included, we are able to quantify the ozone loss occurring *en route* to the receptor. Strong correlations between low ozone concentrations and the spatially integrated footprints from FLEXPART, especially during the period summer to autumn, indicate the importance of the Siberian forests as a sink for tropospheric ozone.

Keywords: tropospheric ozone, Siberian forests, TROICA, YAK, Zotino

1. Introduction

Forests and wetlands act as biological sources and sinks for many atmospheric compounds and, thus, play an important role for the chemical composition of the atmosphere (Gao et al., 1993). Large areas on the Russian territory are covered by boreal forests, tundra and wetlands. Siberia, in particular, stretches over some 8000 km from the Urals at about 60°E to the Pacific Coast at 170°E, and over some 3500 km from the Chinese and Mongolian borders near 48°N to the Arctic islands around 80°N. In total, Siberia encompasses 13.1×10^6 km^2, which is about 9% of the Earth's land area. With only 36 million inhabitants, roughly 0.5% of all people worldwide, Siberia is one of the least populated areas worldwide. Furthermore, almost all people live in the southern parts of Siberia along the Trans-Siberian railway. Of the total area of Siberia, Shvidenko and Nilsson (1994) classified about 48% as forest, which constitutes about 20% of the world's forests in total and about 50% of all coniferous forest areas. Siberia can be divided into three regions: West Siberia, East Siberia, and Far East Siberia. Pine forests dominate in the West and larch forests in the two eastern regions (Shvidenko and Nilsson, 1994).

Large areas, about 20 000 km^2, of Siberian forests are burnt annually by fires, some of them natural, others triggered by humans (Schultz et al., 2008). The areas burned have increased in recent years also because of inefficient fire-control measures and because the resources devoted to fire control are deteriorating significantly in Siberia (Shvidenko and Nilsson, 1994; Flannigan et al., 2009). Forest fires emit a large variety of compounds, including ozone precursors carbon monoxide (CO) and nitrogen oxides (NO$_x$) (Andreae and Merlet, 2001) that play a significant role in atmospheric chemistry.

*Corresponding author.
email: anki.stjernberg@itm.su.se

1

Siberian forest fires emit annually 128 ± 104 TgC yr^{-1} (van der Werf et al., 2010), with a large inter-annual variability (Tanimoto et al., 2000; Wotawa et al., 2001; Derwent et al., 2007).

Tropospheric ozone (O_3) is an important trace gas that plays a key role in tropospheric photochemistry and is the main source of the hydroxyl radical (OH). Recent studies on observed historical and present time ozone mixing ratios show that the background tropospheric ozone mixing ratios have doubled since pre-industrial times due to human activity (Vingarzan, 2004; Monks et al., 2009). There are indications that background ozone levels over the mid-latitudes of the Northern Hemisphere have continued to rise over the past three decades in the range of approximately 0.5–2% per year (Derwent et al., 2007; Parrish et al., 2009; Tanimoto, 2009; Cooper et al., 2010). Tropospheric ozone acts as a greenhouse gas and increases because the pre-industrial era and is estimated to give a radiative forcing of 0.35 ± 0.15 W m^{-2} according to Forster et al., 2007. This is about 20–25% of the estimated total radiative forcing from greenhouse gases (Monks et al., 2009).

An important sink of ozone is its uptake by vegetation both passively by deposition on cuticular (leaf) surfaces and actively by stomatal gas exchange (Altimir et al., 2008). The stomata opening is controlled mainly by light, and stomata are more open during daytime, but are still partly open for many plant species during night (Roberts, 1990). Stomatal opening is also controlled by environmental stresses such as drought and enhanced mixing ratios of air pollutants that will induce stomatal closure (Maier-Maercker and Koch, 1992). Ozone, in particular, is a harmful oxidant that affects the cellular structures in plants. Exposure to ozone and other stresses often leads to increased emissions of biogenic volatile organic compounds (BVOCs) (Loreto et al., 2004; Niinemets, 2010). The emitted BVOCs not only alter the plants' physiological response to ozone but can also react with ozone in the atmosphere, thus destroying the ozone before it reaches the plant surface (Goldstein et al., 2004; Pinto et al., 2010). Thus, BVOC emission is likely a protective mechanism against ozone exposure. Low surface ozone concentrations in large forest areas have been reported both for Siberia (Pochanart et al., 2003) and Amazonia (Kirchhoff, 1988) and have been explained both by the effective dry deposition on leaf surfaces and destruction by BVOCs. Given the globally rising ozone concentrations, these ozone sink areas are very important and deserve more attention.

Recently, low ozone-mixing ratios have been observed from aircraft in the boundary layer (BL) over Siberia during the YAK-Airborne Extensive Regional Observations in Siberia (AEROSIB) campaigns conducted over Siberia during the years 2006–2008 (Paris et al., 2008, Paris et al., 2010a). Ozone mixing ratios there increase rapidly with altitude indicating the importance of the surface as a sink. The vertical gradient in ozone-mixing ratios observed above Siberia is also much steeper in summer when the vegetation is active than in spring. We take these findings as a motivation for this study, in which we investigate measured ozone-mixing ratios over Siberia from three different measurement platforms and research programmes: (1) train measurements performed by the TRans-Siberian Observations Into the Chemistry of the Atmosphere (TROICA) campaigns since the year 1999, (2) aircraft measurements from YAK-AEROSIB campaigns during the years 2006–2008 and (3) measurements made at the Zotino research station. By combining datasets from the three different platforms, each with its own advantages and disadvantages, the spatial and temporal variation of ozone over Siberia can be studied. We investigate the source regions and the role of the Siberian forests as a sink for O_3 by combining the measurements with air mass transport modelling using the dispersion model FLEXPART. This work is performed as part of a joint Norwegian–Russian research program; Study of Russian Air Pollution Sources and their Impact on Atmospheric Composition in the Arctic using the TROICA railway carriage, data from Svalbard and the FLEXPART transport model (RAPSIFACT).

2. Data and methods

2.1. Trace-gas measurements

2.1.1. Station measurements. The remote station Zotino is located in the western part of Siberia (300 m above sea level 60.43°N, 89.40°E, see Fig. 1). The environment of the Zotino region is dominated by pine forests (*Pinus Sylvestris*) interspaced with bogs. The closest cities are situated over 2000 km to the East (Yakutsk) and 1000 km to the West (Surgut) and an industrial area with large nickel smelters is located near Norilsk, about 1000 km to the North. See more information about the experiment region of Zotino in Lloyd et al. (2002) and Schulze et al. (2002). In this study, we use ozone measurements from Zotino from mid-March 2007 to early February 2008. The O_3, NO and NO_2 measurements at Zotino station were performed using correspondingly DASIBI 1008 and TE42C-TL instruments that have been also exploited in TROICA campaigns.

All data were averaged to 3-hourly values for direct matching with FLEXPART data (see below). Even though the measurements covered only 1 yr, they allow studying the seasonal variation of ozone in Siberia, shown in Fig. 2. The highest ozone concentrations are observed in spring, particularly in March and April. This is in agreement with
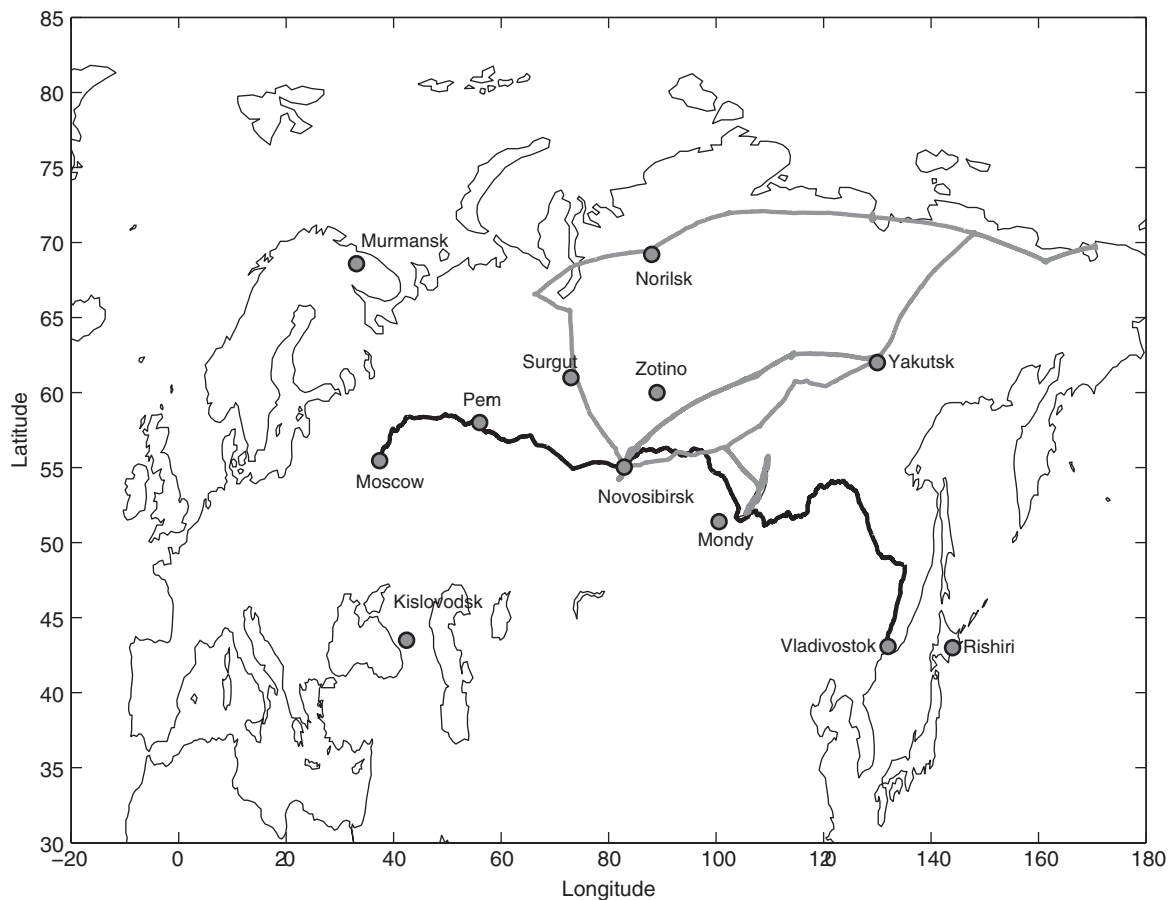
Fig. 1. Map showing the location of the Zotino station and the major cities and the Monday station (circles), the Trans-Siberian railway (black line) and the flight track from the YAK missions (grey line).
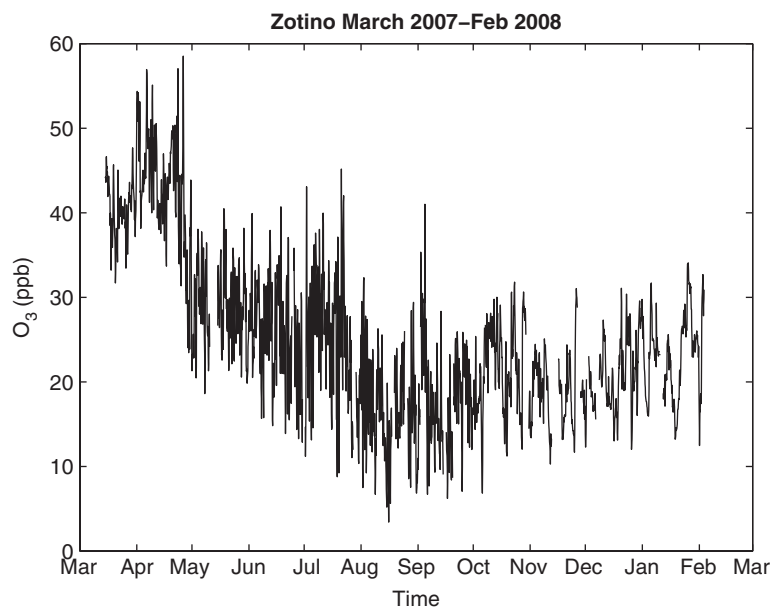

Fig. 2. Seasonal variation of 3-hourly O₃ values measured at Zotino station from mid-March 2007 to early February 2008.

the increasing photochemical ozone production and import from the stratosphere as observed in the high-latitude North American remote free troposphere (FT) during spring (Browell et al., 2003). However, contrary to the free tropospheric observations over North America, ozone concentrations at Zotino start to rapidly decline in May to reach a minimum in autumn. It start increasing again in winter. This behaviour is similar to the seasonality reported for another Siberian surface site, Mondy (Pochanart et al., 2003). However, ozone mixing ratios at Zotino are lower by more than 10 ppbv than those at Mondy, especially in summer, likely because Mondy is located further to the southeast at the fringes of Siberia. In contrast to the Siberian surface observations, aircraft observations suggest a summer maximum in the upper troposphere over Siberia (Stohl et al., 2001). It, thus, appears that the summer minimum near the surface is related to ozone deposition on plant surfaces or chemical destruction with BVOCs near the forest canopy. Based on the observed seasonality, we distinguish between the seasons *spring* (March, April and May), *summer* (June, July and August), *autumn* (September, October and November) and *winter* (December, January and February), also denoted SPR, SUM, AUT and WIN, respectively, in the paper.

2.1.2. Train measurements. Train-based measurements allow us to study the horizontal distribution of ozone over the Eurasian continent. TROICA was established in 1995 (Crutzen et al., 1998) and uses a train carriage as a mobile measurement platform. In total, there have been 15 TROICA campaigns since 1995, of which 11 were running in the East–West direction along the Trans-Siberian railway between Moscow and Vladivostok and three in the North–South direction between Murmansk and Moscow or Kislovodsk. One campaign in 2006 was conducted around Moscow. In the present study, we focus on O_3 measurements obtained during campaigns running from 1999 to 2009 in the East–West direction, in total 7 campaigns (Fig. 1, Table 2). The length of the campaigns is up to 14 d during which the train is travelling first eastwards to Vladivostok and then back to Moscow.

TROICA measurements of interest are those of O_3 and of the nitrogen oxides (NO and NO_2). For O_3, a Dasibi 1008-RS instrument with a measurement interval between 0 and 1000 ppbv and with an accuracy of 1 ppbv was used. The instrument was calibrated against the ozone generator GP-024 and against the European standard SPR no. 011 and Russian national standard SPR no. 038 (e.g. Golitsyn et al. 2002; Elansky 2009). Nitrogen oxide- and nitrogen dioxide-mixing ratios were measured with AC-30M (TROICA-5), TE-42C-TL (TROICA-7, -8, -9) and Teledyne M200AU (TROICA-11, -12, -13) two-channel chemiluminescent gas analysers. The method is based on the luminescence radiation from the chemical reaction between NO and O_3. To measure NO_2, a catalytic converter reducing NO_2 to NO was used. The measurement range is 0–1000 ppbv with an accuracy of 1 ppbv for the AC-30M, 0.05–400 ppbv and 0.05–200 ppbv with the general error1% for the TE-42C-TL and M200AU, respectively. The measurement interval is 10 s, and reference gas mixtures provided by Max Planck Institute for Chemistry (Mainz), Global Monitoring Division of U.S. National Oceanic and Atmospheric Administration (GMD/NOAA) and All-Russian D.I. Mendeleyev Institute for Metrology (VNIIM) in Saint Petersburg were used to calibrate the instruments (Markova et al., 2004; Elansky et al. 2009). In addition to the trace-gas measurements, standard measurements of the meteorological parameters such as temperature, pressure and incoming solar radiation were performed. For more details, see Elansky et al. (2009).

2.1.3. *Airborne measurements.* Finally, we analysed data from five airborne campaigns of the YAK-AEROSIB project (see Paris et al., 2010b, for an overview; Table 1). These campaigns took place over the East and Far East Siberia on a return route between Novosibirsk and Yakutsk (see Fig. 1). During one of the campaigns, in July 2008, an additional circuit was flown further North. During the flights, continuous measurements of carbon monoxide (CO), carbon dioxide (CO_2), O_3 and aerosol concentrations were made. In this study, we analyse the measurements of CO and O_3.

Table 1. Summary of ozone data used in this study

Data source	Platform	Period covered	Measurement technique	Measurement uncertainty	References
TROICA	Train	1999–2009	UV absorption	1 ppbv	Elansky et al. (2009)
YAK-AEROSIB	Aircraft	2006–2008	UV absorption	2 ppbv/2%	Paris et al. (2008)
Zotino	Tower	March 2007–March 2008	UV absorption	1 ppbv	Skorokhod et al. (2008)

Ozone is measured using a Thermo Instruments Model 49 with modifications for internal calibration, and aircraft operations safety was used (Thouret et al., 1998; Paris et al., 2008). The instrument is based on classic UV absorption in two parallel cells, with a precision of 2 ppbv, 2% for an integration time of 4 s. It is compensated for aircraft pressure and temperature variations. Prior to detection, air is pressurised to cabin pressure, using a Teflon KNF Neuberger pump model N735 also used for the CO instrument. The O_3 analyser has been initially calibrated against a NIST-related reference calibrator Model49PS. A calibration box with an O_3 generator is used for laboratory check for the analyser before and after each campaign.

The CO analyser has been described in Nédélec et al. (2003). It is a fully automated instrument designed to reach an accuracy of 5 ppbv or 5%. The instrument is based on a commercial infrared absorption correlation gas analyser (Model 48C, TEI Thermo Environment Instruments). The model 48CTL is qualified by the U.S. EPA-designed method EQSA-0486-060. For more details about the instrumentation, the geographical area studied and campaign descriptions, see Paris et al. (2008).

2.2. Model description

Calculations of the air-mass transport to the measurement locations were made using the Lagrangian particle dispersion model (LPDM) FLEXPART (e.g. Stohl et al. 1998, 2005). Contrary to three-dimensional simple trajectory models, the FLEXPART model takes into account turbulence and convection in the atmosphere. We ran the model 20 d backwards in time with different particle release time intervals for each platform; from the station at 3-hour intervals, from the train at 1-minute intervals and from the aircraft in 10-seconds or 60-seconds intervals depending on available data from each campaign.

FLEXPART uses wind fields from the European Centre for Medium-Range Weather Forecasts (ECMWF) with a resolution of $1° \times 1°$. The model calculates the dispersion of a large number of particles (here, 40 000) that are released at one point for a specific time. The model output of the backward calculations is the so-called potential emission sensitivity (PES) field (unit s m^3 kg^{-1}). For a more detailed explanation of FLEXPART's backward mode, see Stohl et al. (2003) and Seibert and Frank (2004). In this study, we use the PES fields for the lowest 100 m layer (the so-called footprint layer) and for the lowest 3000 m layer (L1). The PES values are a measure for where and how intensively the sampled air mass has been in contact with the surface and, thus, how sensitive the sampled air mass is to surface exchange fluxes.

Calculations of PES were performed for both a passive tracer, for which removal processes are ignored, as well as

for an ozone-like tracer for which dry deposition is accounted for during the transport following the scheme by Wesely (1989). The deposition scheme reduces the PES values for the ozone-like tracer compared to the passive tracer, giving a measure of the possible ozone loss due to dry deposition over the 20 d prior to arrival at the measurement site. We extracted land cover data from the ECMWF at $1° \times 1°$ resolution and aggregate several land cover classes as 'high vegetation' (evergreen needle leaf, deciduous needle leaf, deciduous needle leaf, evergreen broadleaf and mixed woodland). We will later use this classification to compare PES values for all land use classes and only over forest and wetland.

2.3. Statistical analyses

For the analysis of the potential source and sink regions of O_3, we apply a statistical method as described by Hirdman et al. (2010) and which is similar to statistical trajectory analyses. We relate every measurement denoted with index m to a corresponding modelled passive-tracer footprint PES field $S(i,j,m)$, where i and j are indices of the geographical grid on which S is defined. Using all M measurements available, we calculate an average PES value according to

$$S_T(i,j) = \frac{1}{M} \sum_{m=1}^{M} S(i,j,m) \qquad (1)$$

We then select a subset of a number L of observations containing the 25th or 75th percentiles of the concentration distribution and again calculate average PES values for these subsets only, according to

$$S_P(i,j) = \frac{1}{L} \sum_{l=1}^{L} S(i,j,l) \qquad (2)$$

where the suffix P denotes a certain percentile (25th or 75th) of the mixing ratio distribution.

$$R_P(i,j) = \frac{L}{M} \frac{S_P(i,j)}{S_T(i,j)} \qquad (3)$$

Equation (3) can then be used for identifying grid cells that are likely sources (high percentiles) or sinks (low percentiles) of O_3. If air mass transport patterns were the same for the data subset and for the full dataset, we would expect $R_p = 0.25$ for all grid cells (i,j). Information on the sources and sinks of O_3 are contained in the deviations from this expected value. When using the top quartile of the data, for instance, $R_{75}(i,j) > 0.25$ means that high measured O_3 mixing ratios are associated preferentially with high S values in grid cell (i,j), indicating a likely source, whereas $R_{75}(i,j) < 0.25$ indicates a possible sink. Conversely, when

using the lowest quartile of the data, $R_{25}(i,j) > 0.25$ indicates a likely sink in grid cell (i,j), and $R_{25}(i,j) < 0.25$ a source. Not all features of R_P are statistically significant. Spurious R_P values can occur especially where S_T values are low *and*, therefore we limit the calculation of R_P to grid cells, where $S_T > 50\,\text{s}\ \text{m}^3\,\text{kg}^{-1}$. For further details, see Hirdman et al. (2010).

3. Results

We apply the above methods to our different datasets from Siberia. The Trans-Siberian railway covers a distance of about 9000 km, from Moscow (56°N, 38°E) to Vladivostok (43°N, 131°E). Over such a long distance, the mixing ratios of O_3 and its precursors vary considerably as the train passes by cities, industrial and rural areas. As we wish to investigate the variation of ozone due to surface fluxes over Siberia, we are mainly interested in background O_3, not in variations due to fresh anthropogenic emissions of precursors. From Perm (58°N, 56°E) to Vladivostok (Fig. 1), the railroad crosses more rural areas. However, a positive gradient of the total O_3 mixing ratios could be observed from Perm towards the east as the train reaches more polluted areas in Eastern Asia (Elansky 2009).

To remove the influence of fresh emissions prior to further analysis, we filter out the O_3 data for conditions when NO_x mixing ratios are elevated. Based on the results of Elansky et al. (2009), we apply a moderate criterion for background condition for both TROICA and Zotino data; $NO_x < 2.2\,\text{ppbv}$, $NO_x < 1.2\,\text{ppbv}$, $NO_x < 1.4\,\text{ppbv}$ and $NO_x < 2.2\,\text{ppbv}$ for spring, summer, autumn, and winter, respectively. Only between 4 and 23% of the TROICA measurements are obtained under background conditions because the train travels across inhabited areas, whereas this fraction is substantially higher, between 80 and 91%, for the Zotino station, the location of which was specifically chosen to sample background conditions. The background criteria used for the aircraft measurements follow the procedure by Paris et al. (2008) that is based on the CO data. The CO background mixing ratios for each campaign are April 2006 < 167 ppbv, September 2006 < 108 ppbv, August 2007 < 104 ppbv and July 2008 < 101 ppbv.

For further statistical analyses, the airborne O_3 data are divided into two altitude sections designated L1 and L2, respectively. L1 corresponds to altitudes from the surface up to 3000 m, and L2 from 3000 m up to 6500 m. The former loosely represents air masses that likely have recently been within the boundary layer (BL) and, thus, have been influenced by recent direct surface contact and the latter the free troposphere (FT), for which a direct surface contact is unlikely but that may have been in the BL earlier.

Table 2 reports summary statistics for background O_3 for all measurement platforms. It is obvious that there is a strong vertical gradient of O_3 mixing ratios, with station and train data being lower than the aircraft data obtained in the lowest 3000 m, which are in turn lower than ozone mixing ratios measured above 3000 m. The vertical gradient is particularly strong in summer. For instance, we find median ozone mixing ratios of 18–27 ppbv for the Zotino and TROICA data, and 32 ppbv and 67 ppbv for aircraft data obtained below and above 3000 m, respectively. This vertical gradient, best seen in the vertical O_3 profiles shown in Fig. 3, is a strong indication that, in the area studied, the surface acts as a strong sink for O_3 during summer. The vertical O_3 gradients are less strong during other seasons, as shown by Paris et al. (2010a). The higher mixing ratios in the FT are likely sustained by photochemical production in pollution plumes imported from ozone precursor source regions and intrusions of ozone from the stratosphere (e.g. Cooper et al., 2010). Mixing ratios at about 3 km altitude were similar all year round (55–60 ppbv), whereas the lower altitude O_3 mixing ratios observed during the same aircraft campaigns showed a marked spring maximum (~50 ppbv) and summer minimum (~30 ppbv).

To produce statistical analyses of O_3 source and sink regions based on FLEXPART runs as described in Section 2, we divide the O_3 data into two groups: high O_3 (>75th percentile, R_{75}) and low O_3 (<25th percentile, R_{25}) mixing ratios. Figure 4 shows the R_P fields for both low O_3 mixing ratios (R_{25}, left column) and for high O_3 mixing ratios (R_{75}, right column). Data from all three measurement platforms, including both L1 and L2 data from YAK, are here combined for each season.

SPR and SUM show a clear separation between source regions for R_{25} and R_{75}, respectively. Low O_3 mixing ratios correspond to air masses originating not only from higher latitudes: the Arctic, northern parts of Russia and Scandinavia but also from the Pacific Ocean and inner parts of Siberia. It is, thus, clear that low O_3 values in Siberia are associated with intensive surface contact in remote regions during spring and summer. However, it is not clear whether the surface contact over Siberia itself is more important than the surface contact in other remote areas. Some of the low O_3 seems to be associated also with transport from the Arctic where O_3 can be depleted by halogen chemistry in spring (Oltmans, 1981; Bottenheim et al., 1986) and, in summer, with transport with the monsoon flow from the Pacific Ocean. However, notice that the R_P patterns are most robust close to the measurement locations, while they are more uncertain further away, so we think that the forest sink is the most likely explanation for the very low ozone concentrations measured, even if we expect ozone to be low anyway when advected from the Arctic or Pacific Ocean.

Table 2. Summary statistics of background O_3 measurements from the Zotino station, TROICA and YAK-AEROSIB. The aircraft data have further been separated in data obtained below and above 3000 m above sea level

	Min (ppbv)	25%-tile(ppbv)	Median (ppbv)	Mean (std) (ppbv)	75%-tile(ppbv)	Max(ppbv)	Fraction of back-ground data (%)
Zotin—SPR	19	31	39	38(8)	44	59	88
Zotin—SUM	3	17	23	23(7)	28	45	91
Zotin—AUT	6	16	19	19(5)	23	41	80
Zotin—WIN	12	19	22	22(5)	26	34	89
TROICA5 June 1999	1	18	27	28(13)	37	68	23
TROICA7 June–July 2001	1	18	25	26(11)	32	59	18
TROICA8 March–April 2004	16	39	47	44(8)	49	57	17
TROICA9 October 2005	0	18	27	23(10)	30	46	20
TROICA11 July–August 2007	0	13	19	20(9)	26	42	15
TROICA12 July 2008	0	11	18	17(7)	24	29	4
TROICA 13 November 2009	2	19	22	23(6)	26	40	31
YAK—April 2006 Alt < 3000 m	36	45	50	51(5)	55	74	40
YAK—Sept 2006 Alt < 3000 m	21	33	42	45(12)	56	64	36
YAK—Aug 2007 Alt < 3000 m	18	25	30	33(12)	35	68	32
YAK—July 2008 Alt < 3000 m	17	26	33	35(12)	41	85	28
YAK—April 2006 Alt > 3000 m	53	57	60	60(5)	63	86	36
YAK—Sept 2006 Alt > 3000 m	47	54	59	59(7)	64	92	47
YAK—Aug 2007 Alt > 3000 m	33	56	68	65(12)	74	85	29
YAK—July 2008 Alt > 3000 m	28	53	66	67(20)	80	238	33

In contrast, high R_{75} values can be found at lower latitudes: China, central parts of Europe and Russia, the Mediterranean Sea, the Middle East and the regions in the vicinity of the Caspian Sea. Most of these regions have high O_3 precursor emissions and, thus, the high O_3 values are due to long-range transport from these areas. For example, Paris et al. (2010a) showed in their study based on aircraft measurements of O_3 over Siberia a positive correlation between observed O_3 and source regions such as North Eastern China ($R = 0.44$) during summer, European Russia ($R = 0.24$) in spring and Western Europe ($R = 0.35$ and $R = 0.34$) in spring and summer, respectively. Pochanart et al. (2003) have also shown that ozone mixing ratios at Mondy are elevated in air masses arriving from Europe.

For AUT and WIN, low ozone mixing ratios are associated with transport from anthropogenic precursor source regions in Russia and Europe. This is probably a result of the titration of O_3 by NO in polluted areas. Similar results have been observed in a corresponding climatology for the Arctic region (Hirdman et al. 2010). High O_3 mixing ratios in AUT and WIN are associated with transport from lower latitudes such as Southern Europe and Asia. However, results for AUT and WIN must be interpreted with caution because less O_3 data are available and O_3 is also less variable during these seasons.

To quantify the impact of the interaction between the air masses and the surface, we correlate measured O_3 with the spatially integrated (over geographical dimensions I, J) footprint PES fields

$$\text{PES}_{\text{tot}}(m) = \sum_{i=1}^{I} \sum_{j=1}^{J} S(i,j,m) \qquad (4)$$

for the passive tracer. Figure 5 shows a scatter plot between O_3 and PES_{tot}, which reveals a negative correlation
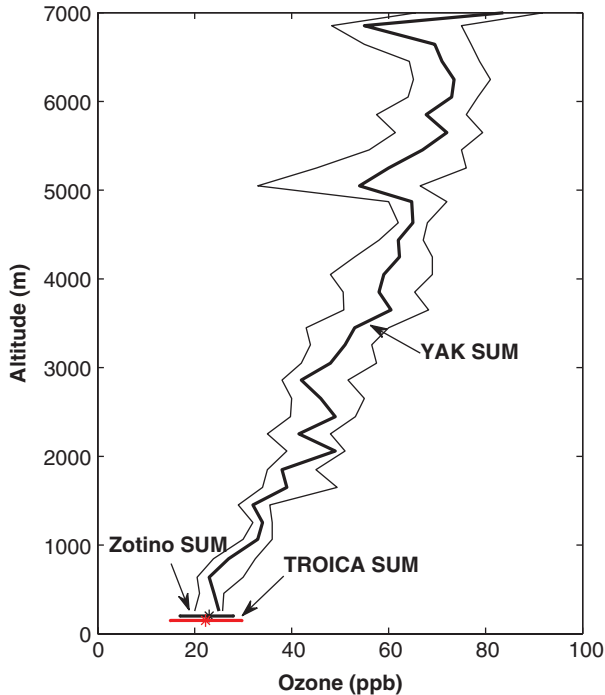
Fig. 3.   Vertical variation (averaged over 200 m altitude bins) of O_3 measured during the YAK summer campaigns. Shown are the median (bold line) as well as the 25th percentile and 75th percentile (thin solid lines). At the bottom, the median, 25th percentile and 75th percentile of summer O_3 data from Zotino (horizontal black line) and from TROICA (horizontal red line) are shown.

throughout the year. This confirms that O^3 mixing ratios are lower when surface contact is strong. Pearson's correlation coefficients, R, with values ranging from -0.26 to -0.89, are largest negative from spring to autumn when O_3 is more variable and when we expect surface interactions to be stronger than during winter. This suggests that O_3 is mainly imported to Siberia as already shown in Fig. 4 and mixing ratios are reduced by surface contact.

Figure 5 also shows scatter plots between O_3 and PES_{tot} only for land cover types forest and wetland, to investigate whether it is mainly the air mass contact with vegetation surfaces that reduces the ozone mixing ratios. Pearson's correlation coefficients are almost the same for this analysis than when calculating PES_{tot} for all land cover types, indicating that depositions over forests and wetlands are mainly responsible for reducing the ozone. Surface contact over other areas (e.g. the Arctic in spring or the maritime BL) is also associated with low O_3 mixing ratios. Still, most of the surface contact especially during the last few days before arrival takes place over forested areas and wetlands and seems to drive the O_3 destruction.

Compared to footprint PES values for the passive tracer, footprint PES values for the ozone-like tracer are reduced by the parameterised dry deposition. Differences are largest when there is a major surface contact (thus, enabling dry deposition) and when conditions are favourable for O_3 deposition. The deposition scheme implemented in FLEX-PART (Wesely, 1989) accounts for variability of the O_3 deposition velocities resulting from different land cover types, state of the vegetation (e.g. parameterised stomatal closure) and meteorological parameters. As for the passive tracer (see eq. 4), we also spatially integrate the footprint PES values for the ozone tracer and denote the integrated quantity PES_{O_3}. The quantity $PES_{tot} - PES_{O_3}$, thus, is a measure of the parameterised deposition rates accumulated backwards over the last 20 d and may be called potential surface deposition. $PES_{tot} - PES_{O_3}$ has large values when integrated footprint emission sensitivity PES_{tot} is large (indicating intense contact of the sampled air mass with the surface) and when PES_{O_3} is small compared to PES_{tot}, indicating that the surface contact took place when parameterised O_3 dry deposition was strong. $PES_{tot} - PES_{O_3}$ has zero values either when the air mass had no surface contact ($PES_{tot} = 0$ and $PES_{O_3} = 0$) or when there was surface contact but no parameterised deposition ($PES_{O_3} = PES_{tot}$). In reality, if there is surface contact, there will always be O_3 deposition, but deposition velocities can be very small, for instance during night time when stomata are closed and atmospheric stability is high, or over snow and water surfaces.

Figure 6 shows measured O_3 as a function of the logarithm of $PES_{tot} - PES_{O_3}$. As for the scatter plot against PES_{tot}, O_3 values decrease with increasing values of $PES_{tot} - PES_{O_3}$. As expected, the relationship is nearly linear when O_3 is graphed against the logarithm of $PES_{tot} - PES_{O_3}$. This confirms that the O_3 loss rate (expressed as ozone lost per time interval per unit of ozone present) is proportional to $PES_{tot} - PES_{O_3}$. For values of $PES_{tot} - PES_{O_3} > 4 \times 10^4$ s m^3 kg^{-1}, measured O_3 mixing ratios are very low for the season for all seasons. For instance, for $PES_{tot} - PES_{O_3} > 4 \times 10^4$ s m^3 kg^{-1}, all measured O_3 values are below 20 ppbv in autumn. This means that air masses that are exposed to strong dry deposition in the region (because of high deposition velocities, a prolonged exposure of the air mass to the surface or, most effectively, a combination of both) will eventually lose most of their O_3, regardless of their initial ozone mixing ratio imported to Siberia.

4. Conclusions

In the present study, we have analysed ozone mixing ratios in the troposphere in Siberia with respect to air-mass transport. We have used ozone measurements collected from three
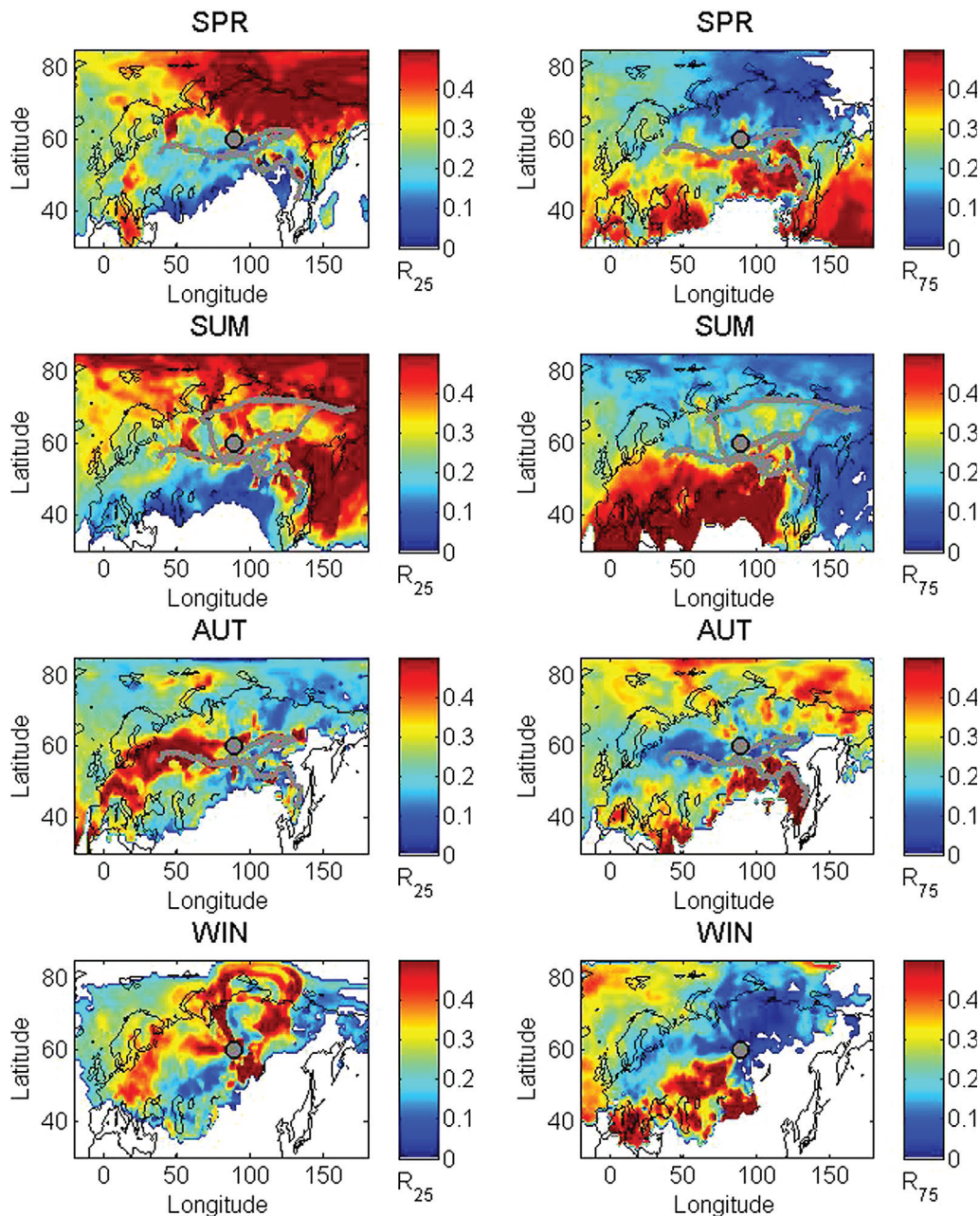
Fig. 4. R_P for ozone data from Zotino, TROICA campaigns, and YAK campaigns combined and divided into spring (SPR), summer (SUM), autumn (AUT), and winter (WIN) (shown from top to bottom, respectively). The panels on the left-hand side show results for low ozone mixing ratios ($<$25th percentile, R_{25}) and the panels on the right-hand side show results for high ozone mixing ratios ($>$75 th percentile, R_{75}). The grey dot indicates the position of the Zotino station, and the grey lines show the tracks for the Trans-Siberian railway and the aircraft flights (cf. Fig. 1). Notice that for winter, only data from Zotino were available.

different measurement platforms: (1) a train carriage along the Trans-Siberian railway between Moscow and Vladivostok (TROICA), (2) continuous measurements from the Zotino station located in western part of Siberia and (3) airborne measurements over Siberia performed during the years 2006–2008 (YAK-AEROSIB). Data were grouped

into season, and particular attention was paid to the period from spring to autumn when the vegetation is active.

The main objective of the study has been to investigate the importance of the Siberian forests acting as a sink for ozone and quantitatively determine the impact of this sink on the measured ozone mixing ratios in the region. To
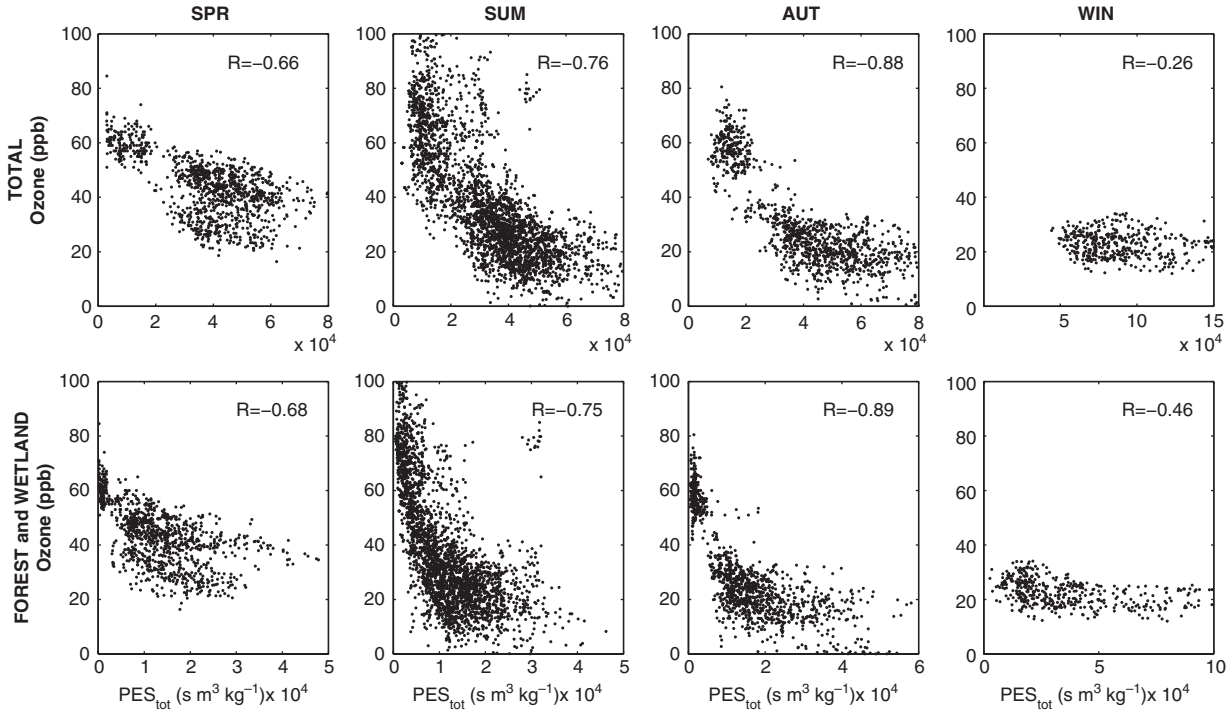
Fig. 5.   Ozone (ppbv) as a function of the potential emission sensitivity (PES) ($s\,kg^{-1}\,m^3$) and the correlation R for station, train, and aircraft data. The upper row of panels show the total PES and the lower row of panels show the PES only for forest and wetland. Data are separated between the seasons SPR, SUM, AUT, and WIN.

determine the strength of the surface sink for ozone, we calculate the footprint PES using 20-d backward simulations with the Lagrangian dispersion model FLEXPART. Footprint PES was used in the past to quantify the sensitivity of a sampled air mass to receiving emission input from surface sources. However, here it is used to

quantify the sensitivity to surface deposition fluxes of ozone. We first used the PES fields for a statistical analysis of the source and sink regions for ozone measured in Siberia. Further on, we performed a statistical analysis of the dependence of measured ozone mixing ratios on the total spatially integrated footprint PES. In addition, we
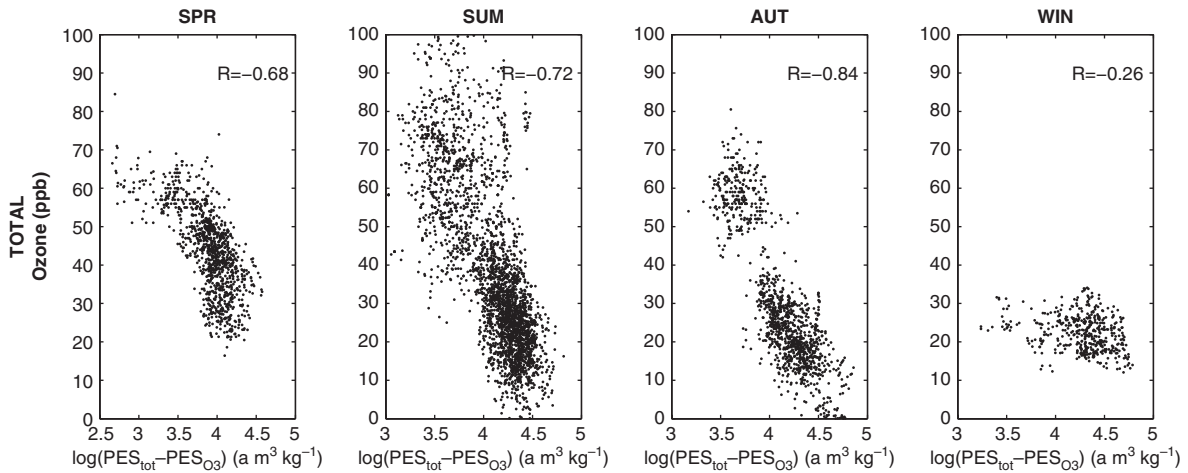

Fig. 6.   Ozone (ppbv) as a function of the surface interaction as expressed by the function of $PES_{tot} - PES_{O_3}$ ($s\,kg^{-1}\,m^3$) and the correlation, R, shown in logarithmic scale for station, train and aircraft data. Data are separated between the seasons SPR, SUM, AUT, and WIN.

also performed FLEXPART backward simulations for an ozone-like tracer that was subject to dry deposition. The difference between PES values for the passive and the ozone-like tracer is a measure of the potential for loss of ozone through dry deposition and can be compared with measured ozone mixing ratios.

Our conclusions from this study are:

- The statistical analysis of the ozone source/sink regions shows that, for all measurement platforms (station, train and aircraft), low ozone mixing ratios are related to advection from relatively clean regions, such as the Arctic and the Pacific Ocean, followed by near-surface transport across Siberia. Source regions for ozone are found South of the measurement locations throughout the year, which are related to advection of air masses from ozone precursor source regions (e.g. China, Europe).
- Comparison of vertical ozone profiles obtained from aircraft measurements, surface station and train measurements in Siberia shows a strong reduction of ozone from the free troposphere towards the surface, particularly during the summer. For instance, we find median summer-time ozone mixing ratios measured by aircraft of 67 ppbv between 3000 and 6500 m, 32 ppbv below 3000 m and only 18–27 ppbv for the station and train data. This vertical gradient suggests a strong surface sink of the ozone.
- To further quantify the surface sink, we correlated the spatially integrated footprint emission sensitivities from FLEXPART with measured ozone mixing ratios. We found negative correlations, with the lowest ozone mixing ratios for the strongest surface contact. The correlations are strongest during spring, summer and autumn. This indicates that surface contact, mainly over Siberia, leads to a dramatic reduction of ozone, explaining also the low overall surface ozone concentrations measured in Siberia especially during the summer.
- For further analysis of the deposition sink, we correlated measured ozone with a model quantity that measures the accumulated effect of parameterised potential surface deposition of the sampled air masses during the last 20 d before arrival at the station. For high values of the potential surface deposition, only very low measured ozone mixing ratios are found, typically below 20 ppbv. This indicates that an air mass in contact with the Siberian land surface will eventually lose most of its ozone, regardless of the initial ozone content of the air mass before it entered Siberia. This again emphasises the importance of the surface loss of ozone over Siberia.

We should point out that although we attributed the ozone loss to parameterised dry deposition, in reality some of the ozone loss may be due to chemical destruction in the clean Siberian boundary layer, particularly related to the emissions of BVOCs. BVOC emissions and associated ozone destruction may be strongly correlated with ozone dry deposition (for instance, both are higher during daytime than during night time and both require surface contact) and, thus, the two mechanisms cannot be separated in our analyses, which is a major caveat. Nevertheless, both mechanisms are related to the Siberian forests, emphasising the importance of Siberia as an ozone sink. Because of its large area, Siberia is relevant for the ozone budget also on a global scale.

Siberia is currently covered with large areas of wetlands and tundra and is a pristine area with negligible anthropogenic ozone precursor emissions. However, changes could be brought about in the future by increasing anthropogenic emissions (e.g. due to enhanced oil drilling or population growth) and by climate change. The ecology of the Siberian forests and, thus, biogenic emissions and surface deposition may change with a changing climate. Furthermore, increasing ozone concentrations imported from precursor regions may damage the Siberian forests. All these changes could reduce the current strength of the O_3 sink in Siberia. Increasing O_3 concentrations could furthermore trigger a positive feedback mechanism via reduced loss of ozone in Siberia. These changes would be of relevance for the entire Northern hemisphere.

5. Acknowledgements

References

Altimir, N., Kolari, P., Tuovinen, J.-P., Bäck, J., Suni, T. and co-authors. 2008. Foliage surface ozone deposition: a role for surface moisture? *Biogeosciences* **3**, 209–228.

Andreae, M. O. and Merlet, P. 2001. Emission of trace gases and aerosols from biomass burning. *Glob. Biogeochem. Cy.* **15**, 955–966.

Bottenheim, J. W., Gallant, A. G. and Brice, K. A. 1986. Measurements of NOY species and O3 at 82°N latitude. *Geophys. Res. Lett.* **13**, 113–116.

Browell, E. V., Hair, J. W., Butler, C. F., Grant, W. B., DeYoung, R. J. and co-authors. 2003. Ozone, aerosol, potential vorticity, and trace gas trends observed at high-latitudes over North

America from February to May 2000. *J. Geophys. Res.* **108**, 8369.

Cooper, O. R., Parrish, D. D., Stohl, A., Trainer, M., Nédélec, P. and co-authors. 2010. Increasing springtime ozone mizing ratios in the free troposphere over western North America. *Nature* **463**, 344–348.

Crutzen, P. J., Elansky, N. F., Hahn, M., Golitsyn, G. S., Brenninkmeijer, C. A. M. and co-authors. 1998. Trace gas measurements between Moscow and Vladivostok using the Trans-Siberian railroad. *J. Atmos. Chem.* **29**, 179–194.

Derwent, R. G., Simmonds, P. G., Manning, A. J. and Spain, T. G. 2007. Trends over a 20-year period from 1987–2007 in surface ozone at the atmospheric research station, Mace Head, Ireland. *Atmos. Environ.* **41**, 9091–9098.

Elansky, N. F. 2009. Russian studies of the Atmospheric ozone in 2003–2006. *Izv. Atmos. Ocean. Phys.* **45**, 207–220.

Elansky, N. F., Belikov, I. B., Berezina, E. V., Brenninkmeijer, C. A. M., Buklikova, N. N. and co-authors. 2009. *Atmospheric composition observations over Northern Eurasia using the mobile laboratory: TROICA experiments.* The International Scientific and Technology Center, Moscow, 73 p.

Flannigan, M. D., Stocks, B., Turetsky, M. and Wotton, B. M. 2009. Impacts of climate change on fire activity and fire management in the circumboreal forest. *Glob. Change Biol.* **15**, 549–560.

Forster, P., Ramaswamy, V., Artaxo, P., Berntsen, T., Betts, R. and co-authors. 2007. Changes in atmospheric constituents and in radiative forcing. In: *Climate Change 2007: The Physical Science Basis. Contribution of Working Group I to the Fourth Assessment Report of the Intergovernmental Panel on Climate Change* (eds S. Solomon, D. Qin, M. Manning, Z. Chen, M. Marquis and co-authors). Cambridge University Press, Cambridge United Kingdom and New York, NY, USA.

Gao, W., Wesely, M. L. and Doskey, P. V.1993. Numerical modeling of the turbulent diffusion and chemistry of NO_x, O3, isoprene, and other reactive trace gases in and above a forest canopy. *J. Geophys. Res.* **98**, 18,339–18,353.

Goldstein, A. H., McKay, M., Kurpius, M. R., Schade, G. W., Lee, A. and co-authors. 2004. Forest thinning experiment confirms ozone deposition to forest canopy is dominated by reaction with biogenic VOCs. *Geophys. Res. Let.* **31**, L22106, doi:10.1029/2004GL021259.

Golitsyn, G. S., Elansky, N. F., Markova, T. A. and Panin, L. V. 2002. Surface ozone behavior over continental Russia. Izv. Atmos. Ocean. *Phys.* **38**, 116–126.

Hirdman, D., Sodermann, H., Eckhardt, S., Burkhart, J. F., Jefferson, A. and co-authors. 2010. Source identification of short-lived air pollutants in the Arctic using statistical analysis of measurement data and particle dispersion model output. *Atmos. Chem. Phys.* **10**, 669–693.

Kirchhoff, V. W. J. H. 1988. Surface ozone measurements in Amazonia. *J. Geophys. Res.* **93**, 1469–1476.

Lloyd, J., Langenfelds, R. L., Francey, R. J., Gloor, M., Tchebakova, N. M. and co-authors. 2002. A trace-gas climatology above Zotino, central Siberia. *Tellus* **54B**, 749–767.

Loreto, F., Pinelli, P., Manes, F. and Kollist, H. 2004. Impact of ozone on monoterpene emissions and evidence for an isoprene-like antioxidant action of monoterpenes emitted by *Quercus.ilex* leaves. *Tree Physiol.* **24**, 361–367.

Maier-Maercker, U. and Koch, W. 1992. The effect of air pollution on the mechanism of stomatal control. *Trees-Struct. Funct.* **7**(1), 12–25.

Markova, T. A., Elansky, N. F., Belikov, I. B., Grisenko, A. M. and Sevast'yanov, V. V. 2004. Distribution of nitrogen oxides in the atmospheric surface layer over continental Russia. *Izv. Atmos. Ocean. Phys.* **40**(6), 811–813.

Monks, P. S., Granier, C., Fuzzi, S., Stohl, A., Williams, M. L. and co-authors. 2009. Atmospheric composition change—global and regional air quality. *Atmos. Environ.* **43**, 5268–5350.

Nédélec, P., Cammas, J.-P., Thouret, V., Athier, G., Cousin, J.-M. and co-authors. 2003. An improved infrared carbon monoxide analyser for routine measurements aboard commercial Airbus aircraft: technical validation and first scientific results of the MOZAIC III programme. *Atmos. Chem. Phys.* **3**, 1551–1564.

Niinemets, Ü. 2010. Mild versus severe stress and BVOCs: thresholds, priming and consequences. *Trends Plant. Sci.* **15**(3), 145–153.

Oltmans, S. J. 1981. Surface ozone measurements in clean air. *J. Geophys. Res.* **86**, 1174–1180.

Paris, J.-D., Ciais, P., Nédélec, P., Ramonet, M., Belan, B. D. and co-authors. 2008. The YAK-AEROSIB transcontinental aircraft campaigns: new insights on the transport of CO_2, CO and O3 across Siberia. *Tellus* **60B**, 551–568.

Paris, J.-D., Stohl, A., Ciais, P., Nédélec, P., Belan, B. D. and co-authors. 2010a. Source-receptor relationships for airborne measurements of CO_2, CO and O3 above Siberia: a cluster-based approach. *Atmos. Chem. Phys.* **10**, 1671–1687.

Paris, J.-D., Ciais, P., Nédélec, P., Stohl, A., Belan, B. D. and co-authors. 2010b. Transcontinental flights over Siberia: overview of first results from the YAK AEROSIB project. *Bull. Amer. Met. Soc.* **91**, 625–641.

Parrish, D. D., Millet, D. B. and Goldstein, A. H. 2009. Increasing ozone in marine boundary layer inflow at the West coasts of North America and Europe. *Atmos. Chem. Phys.* **9**, 1303–1323.

Pinto, D. M., Blande, J. D., Souza, S. R., Nerg, A.-M. and Holopainen, J. K. 2010. Plant volatile organic compounds (VOCs) in ozone (O_3) polluted atmospheres: the ecological effects. *J. Chem. Ecol.* **36**, 22–34.

Pochanart, P., Akimoto, H., Kajii, Y., Kajii, Y., Potekin, V. M. and Khodzher, T. V. 2003. Regional background ozone and carbon monoxide variations in remote Siberia/East Asia. *J. Geophys. Res.* **108**, 4028.

Roberts, B. 1990. What is stomata and how do they work? *J. Arboric.* **16**(12), 331.

Schulze, E.-D., Vygodskaya, N. N., Tchebakova, N. M., Czimczik, C. I., Kozlov, D. N. and co-authors. 2002. The Eurosiberian Transect: an introduction to the experimental region. *Tellus* **54B**, 421–428.

Schultz, M. G., Heil, A., Hoelzemann, J. J., Spessa, A., Thonicke, K., Goldammer, J. G., Held, A. C., Pereira, J. M. C. and van het Bolscher, M. 2008. Global wildland fire emissions from 1960 to 2000. Global Biogeochem. *Global Biogeochem. Cy.* **22**, doi:10.1029/2004GL021259.

Seibert, P. and Frank, A. 2004. Source-receptor matrix calculation with a Lagrangian particle dispersion model in backward mod. *Atmos. Chem. Phys.* **4**, 51–63.

Shvidenko, A. and Nilsson, S. 1994. What do we know about the Siberian forests? *Ambio* **23**, 396–404.

Skorokhod, A. I., Elansky, N. F., Pankratova, N. V., Vivchar, N. V. and Moiseenko, K. B.2008. Measurements of trace gases at ZOTTO Tall Tower in Central Siberia. *Abstracts of All-Russian Scientific Conference "Research of lower atmosphere processes using tall constructions", Obninsk, October, 8–10*, pp. 117–120 (in Russian).

Stohl, A., Forster, C., Eckhardt, S., Spichtinger, N., Huntrieser, H. and co-authors. 2003. A backward modeling study of intercontinental pollution transport using aircraft measurements. *J. Geophys. Res.* **108**, 4370, doi:10.1029/2002JD002862.

Stohl, A., Forster, C., Frank, A., Seibert, P. and Wotawa, G. 2005. Technical Note: the Lagrangian particle dispersion model FLEXPART version 6.2. *Atmos. Chem. Phys.* **5**, 2461–2474.

Stohl, A., Hittenberg, M. and Wotawa, G. 1998. Validation of the Lagrangian particle dispersion model FLEXPART against large-scale tracer experiment data. *Atmos. Environ.* **32**, 4245–4256.

Stohl, A., James, P., Forster, C., Spichtinger, N., Marenco, A. and co-authors. 2001. An extension of measurements of ozone and water vapor by airbus in-service aircraft (MOZAIC) ozone climatologies using trajectory statistics. *J. Geophys. Res.* **106**, 27,757,768.

Tanimoto, H., Kajii, Y., Hirokawa, J. and Akimoto, H. 2000. The atmospheric impact of boreal forest fires in far eastern Siberia on the seasonal variation of carbon monoxide: observations at Rishiri, a northern remote island in Japan. *Geophys. Res. Let.* **27**(24), 4073–4076.

Tanimoto, H. 2009. Increase in springtime tropospheric ozone at a mountainous site in Japan for the period 1998–2006. *Atmos. Environ.* **43**, 1358–1363.

Thouret, V., Mareco, A., Logan, J. A., Nédélec, P. and Grouhel, C. 1998. Comparisons of ozone measurements from the MOZAIC airborne program and the ozone sounding network at eight locations. *J. Geophys. Res.* **103**, 25,695–25,720.

Vingarzan, R. 2004. A review of surface ozone background levels and trends. *Atmos. Environ.* **38**, 3431–3442.

van der Werf, G. R., Randerson, J. T., Giglio, L., Collatz, G. J., Mu, M. and co-authors. 2010. Global fire emissions and the contribution of deforestation, savanna, forest, agricultural, and peat fires (1997–2009). *Atmos. Chem. Phys.* **10**, 11707–11735.

Wesely, M. L. 1989. Parameterization of surface resistances to gaseous dry deposition in regional-scale numerical models. *Atmos. Environ.* **23**, 1293–1304.

Wotawa, G., Novelli, P. C., Trainer, M. and Granier, C. 2001. Inter-annual variability of summertime CO concentrations in the Northern Hemisphere explained by boreal forest fires in North America and Russia. *Geophys. Res. Let.* **28**, 4575–4578.